

Isomers and polymorphs of (*E,E*)-1,4-bis(nitrophenyl)-2,3-diaza-1,3-butadienes

Christopher Glidewell,^{a*} John N. Low,^b Janet M. S. Skakle^b and James L. Wardell^c

^aSchool of Chemistry, University of St Andrews, St Andrews, Fife KY16 9ST, Scotland,

^bDepartment of Chemistry, University of Aberdeen, Meston Walk, Old Aberdeen AB24 3UE, Scotland, and ^cInstituto de Química, Departamento de Química Inorgânica, Universidade Federal do Rio de Janeiro, CP 68563, 21945-970 Rio de Janeiro-RJ, Brazil

Correspondence e-mail: cg@st-andrews.ac.uk

Received 28 February 2006

Accepted 20 April 2006

The structures of five of the possible six isomers of (*E,E*)-1,4-bis(nitrophenyl)-2,3-diaza-1,3-butadiene are reported, including two polymorphs of one of the isomers. (*E,E*)-1,4-Bis(2-nitrophenyl)-2,3-diaza-1,3-butadiene, C₁₄H₁₀N₄O₄ (I), crystallizes in two polymorphic forms (*Ia*) and (*Ib*) in which the molecules lie across centres of inversion in space groups *P2₁/n* and *P2₁/c*, respectively: the molecules in (*Ia*) and (*Ib*) are linked into chains by aromatic $\pi \cdots \pi$ stacking interactions and C—H $\cdots\pi$ (arene) hydrogen bonds, respectively. Molecules of (*E,E*)-1-(2-nitrophenyl)-4-(3-nitrophenyl)-2,3-diaza-1,3-butadiene (II) are linked into sheets by two independent C—H \cdots O hydrogen bonds. The molecules of (*E,E*)-1,4-bis(3-nitrophenyl)-2,3-diaza-1,3-butadiene (III) lie across inversion centres in the space group *P2₁/n*, and a combination of a C—H \cdots O hydrogen bond and a $\pi \cdots \pi$ stacking interaction links the molecules into sheets. A total of four independent C—H \cdots O hydrogen bonds link the molecules of (*E,E*)-1-(3-nitrophenyl)-4-(4-nitrophenyl)-2,3-diaza-1,3-butadiene (IV) into sheets. In (*E,E*)-1,4-bis(4-nitrophenyl)-2,3-diaza-1,3-butadiene (V) the molecules, which lie across centres of inversion in the space group *P2₁/n*, are linked by just two independent C—H \cdots O hydrogen bonds into a three-dimensional framework.

1. Introduction

We have recently reported the supramolecular structures of the three isomeric (*E,E*)-1-(2-iodophenyl)-4-(nitrophenyl)-2,3-diaza-1,3-butadienes (Glidewell, Low, Skakle & Wardell, 2005). In this series, the 2-nitro isomer forms chains, the 3-nitro isomer forms a three-dimensional framework structure, while the 4-nitro isomer forms a sheet structure. In each isomer, a different array of direction-specific intermolecular interactions is manifest: an iodo \cdots nitro interaction in the 2-nitro isomer, C—H \cdots O and C—H \cdots I hydrogen bonds and aromatic $\pi \cdots \pi$ stacking interactions in the 3-nitro isomer, and a C—H \cdots O hydrogen bond and an iodo \cdots nitro interaction in the 4-nitro isomer. Intrigued by the changes in intermolecular interactions and the corresponding structural changes consequent upon a simple positional change of a single substituent, we have developed the earlier study to an even simpler series of positional isomers, namely the isomeric (*E,E*)-1,4-bis(nitrophenyl)-2,3-diaza-1,3-butadienes, O₂NC₆H₄CH=N—N=CHC₆H₄NO₂, and again we observe wide structural variation. We report here the molecular and supramolecular structures of five of the possible six isomeric 1,4-bis(nitrophenyl)-2,3-diaza-1,3-butadienes, compounds (I)–(V) (see Scheme, and Figs. 1–6) and, in addition, we have identified two polymorphs of 1,4-bis(2-nitrophenyl)-2,3-diazabutadiene (I) (Figs. 1 and 2), but we have consistently failed in attempts

to synthesize the sixth isomer 1-(2-nitrophenyl)-4-(4-nitrophenyl)-2,3-diaza-1,3-butadiene (VI). Both polymorphs of (I) are monoclinic, but their *b*-axis vectors differ by a factor of more than two: we denote the polymorph with the shorter *b* axis as (Ia) and that with the longer *b* axis as (Ib). The structure of the polymorph denoted here as (Ia) was determined some years ago (Hsu *et al.*, 1993) using ambient-temperature diffraction data: however, no discussion of the supramolecular aggregation was given; in particular, the occurrence of the $\pi \cdots \pi$ stacking interactions (see §3.2.1) went unreported.

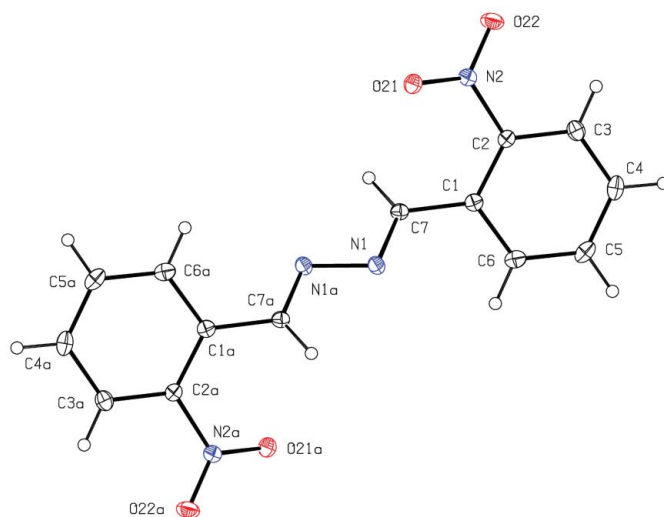
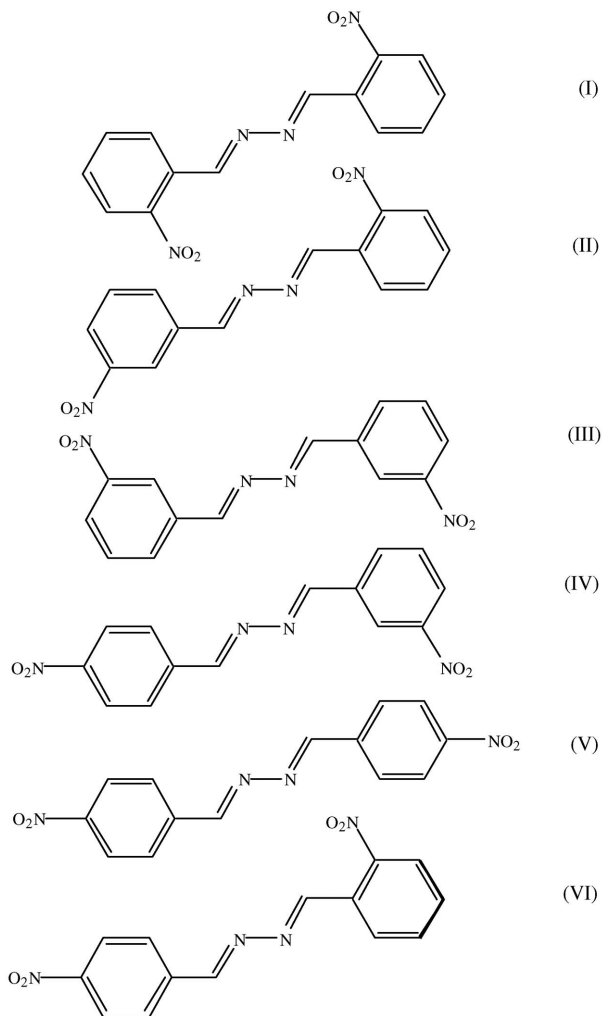


Figure 1
The molecule of polymorph (Ia) showing the atom-labelling scheme. Displacement ellipsoids are drawn at the 30% probability level, and the atoms marked with 'a' are at the symmetry position ($1 - x$, $1 - y$, $1 - z$).

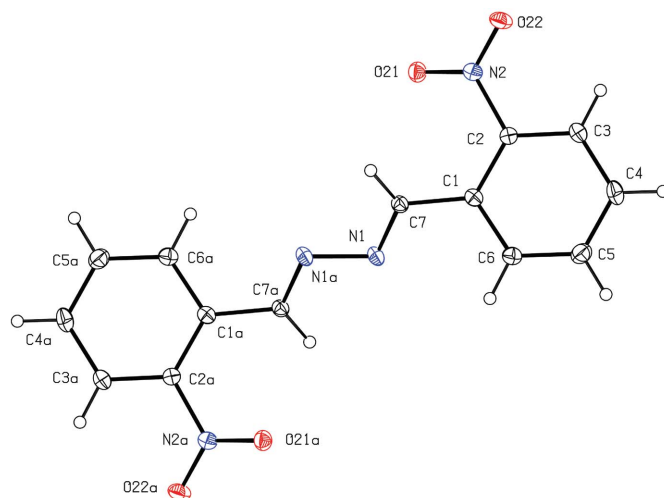


Figure 2
The molecule of polymorph (Ib) showing the atom-labelling scheme. Displacement ellipsoids are drawn at the 30% probability level, and the atoms marked with 'a' are at the symmetry position ($1 - x$, $1 - y$, $1 - z$).

2. Experimental

2.1. Synthesis

Isomers (Ia), (III) and (V) were obtained by heating under reflux a mixture of the appropriate nitrobenzaldehyde (3 mmol) and hydrazine hydrate (1.5 mmol) in methanol (20 cm³) for 30 min, and then leaving the reaction solution at room temperature for 24 h. The products were collected and recrystallized from 1,2-dichloroethane: m.p.s (Ia) 483–486 K, (III) 475–477 K, (V) >500 K. Similar reactions of 3-nitro-

benzaldehyde hydrazone with 2-nitro- or 4-nitrobenzaldehyde yielded isomers (II) and (IV); (II) was recrystallized from methanol, m.p. 471–473 K after partial liquifaction at 421–423 K; (IV) was recrystallized from 1,2-dichloroethane, m.p. 480–483 K. Polymorph (Ib) was isolated by recrystallization, from 1,2-dichloroethane, of the initial product obtained by reaction of 2-nitrobenzaldehyde hydrazone and 2-iodobenzaldehyde, m.p. 443–446 K, following loss of crystallinity at 423 K. Despite the reasonably straightforward preparations of the 2,3' and 3,4' isomers (II) and (IV), numerous attempts to prepare a sample of the 2,4' isomer (VI) (see Scheme) have consistently proved fruitless: using either the reaction of 2-nitrobenzaldehyde with 4-nitrobenzaldehyde hydrazone, or

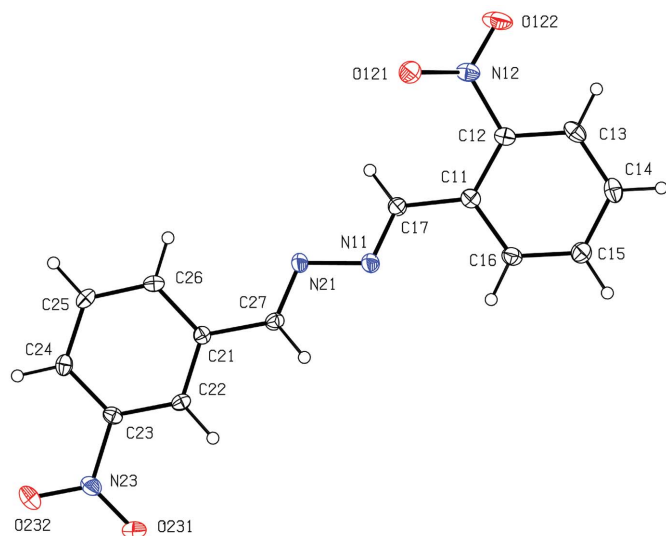


Figure 3
The molecule of isomer (II) showing the atom-labelling scheme. Displacement ellipsoids are drawn at the 30% probability level.

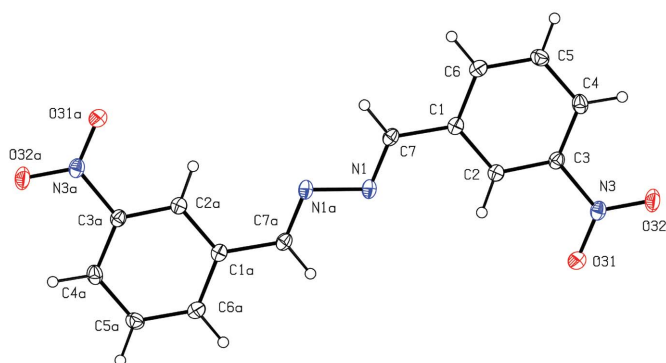


Figure 4
The molecule of isomer (III) showing the atom-labelling scheme. Displacement ellipsoids are drawn at the 30% probability level, and the atoms marked with 'a' are at the symmetry position ($1 - x, 1 - y, 1 - z$).

that of 4-nitrobenzaldehyde with 2-nitrobenzaldehyde hydrazone, the only crystalline products obtained were the symmetrical isomers (I) and (V). The reasons for this behaviour, so different from that in the preparations of isomers (II) and (IV), are entirely unclear.

2.2. Data collection, structure solution and refinement

Diffraction data for compounds (I)–(III) and (V) were collected at 120 (2) K using a Nonius–Kappa CCD diffractometer; in all these cases graphite-monochromated Mo $K\alpha$ radiation ($\lambda = 0.71073 \text{ \AA}$) was employed. Data for (IV) were collected at 120 (2) K using a Bruker SMART APEX2 diffractometer and synchrotron radiation ($\lambda = 0.6778 \text{ \AA}$). Other details of cell data, data collection and refinement are summarized in Table 1, together with details of the software employed.

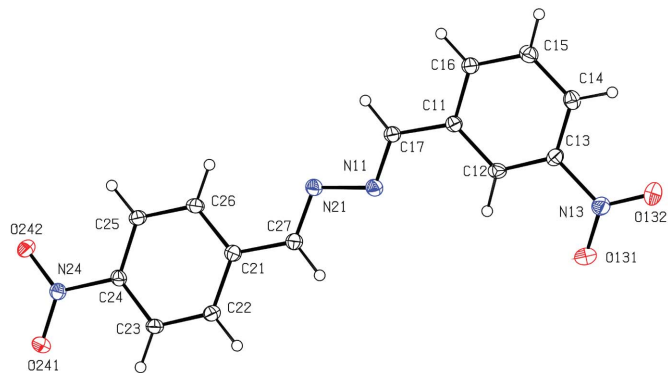


Figure 5
The molecule of isomer (IV) showing the atom-labelling scheme. Displacement ellipsoids are drawn at the 30% probability level.

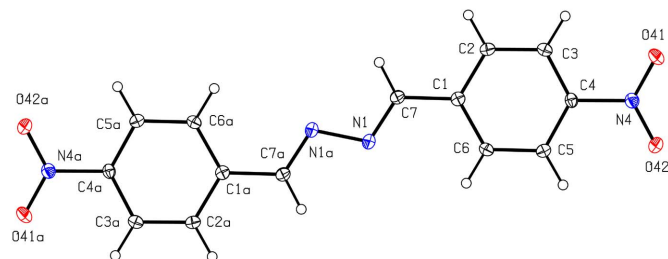


Figure 6
The molecule of isomer (V) showing the atom-labelling scheme. Displacement ellipsoids are drawn at the 30% probability level, and the atoms marked with 'a' are at the symmetry position ($1 - x, 1 - y, 1 - z$).

For each of (Ia), (III) and (V), the space group $P2_1/n$ was uniquely assigned from the systematic absences; likewise the space group $P2_1/c$ was uniquely assigned for (Ib). For isomer (II) the systematic absences permitted $P2_1$ and $P2_1/m$ as possible space groups: from a consideration of the unit-cell volume and the likely value of Z , the space group $P2_1$ was selected and subsequently confirmed by the structure analysis. For isomer (IV), the systematic absences permitted Cc and $C2/c$ as possible space groups: $C2/c$ was selected and subsequently confirmed by the structure analysis.

The structures were solved by direct methods and refined with all data on F^2 . A weighting scheme based upon $P = [F_o^2 + 2F_c^2]/3$ was employed in order to reduce statistical bias (Wilson, 1976). All H atoms were located from difference maps and then treated as riding atoms with C–H distances of 0.95 \AA and with $U_{\text{iso}}(\text{H}) = 1.2U_{\text{eq}}(\text{C})$. In the absence of significant anomalous dispersion, the Flack parameter (Flack, 1983) for (II) was inconclusive (Flack & Bernardinelli, 2000): hence the Friedel-equivalent reflections were merged prior to the final refinements and it was not possible to determine the correct orientation of the structure relative to the polar-axis direction (Jones, 1986). In isomer (Ib), the maximum residual density, 1.438 e \AA^{-3} , is located 0.93 \AA from the C4 atom, lying almost equidistant from H4 and H5, while the largest hole, $-0.306 \text{ e \AA}^{-3}$, is located 0.62 \AA from N2: no plausible disorder model can be developed to take account of these extrema.

Table 1
Experimental table.

	(Ia)	(Ib)	(II)
Crystal data			
Chemical formula	C ₁₄ H ₁₀ N ₄ O ₄	C ₁₄ H ₁₀ N ₄ O ₄	C ₁₄ H ₁₀ N ₄ O ₄
<i>M_r</i>	298.26	298.26	298.26
Cell setting, space group	Monoclinic, <i>P2₁/n</i>	Monoclinic, <i>P2₁/c</i>	Monoclinic, <i>P2₁</i>
Temperature (K)	120 (2)	120 (2)	120 (2)
<i>a</i> , <i>b</i> , <i>c</i> (Å)	9.1379 (4), 6.1776 (3), 11.7682 (4)	7.7809 (2), 14.7825 (6), 6.2196 (2)	7.8036 (2), 7.0914 (3), 12.3424 (4)
β (°)	93.853 (3)	113.106 (2)	101.742 (2)
<i>V</i> (Å ³)	662.82 (5)	658.00 (4)	668.72 (4)
<i>Z</i>	2	2	2
<i>D_x</i> (Mg m ⁻³)	1.494	1.505	1.481
Radiation type	Mo <i>K</i> α	Mo <i>K</i> α	Mo <i>K</i> α
No. of reflections for cell parameters	1511	1503	1653
θ range (°)	3.5–27.5	3.2–27.5	3.3–27.5
μ (mm ⁻¹)	0.11	0.11	0.11
Crystal form, colour	Block, yellow	Block, yellow	Blade, orange
Crystal size (mm)	0.46 × 0.34 × 0.18	0.48 × 0.22 × 0.08	0.50 × 0.32 × 0.12
Data collection			
Diffraction	Bruker–Nonius 95 mm CCD camera on κ -goniostat	Bruker–Nonius 95 mm CCD camera on κ -goniostat	Bruker–Nonius 95 mm CCD camera on κ -goniostat
Data collection method	φ and ω scans	φ and ω scans	φ and ω scans
Absorption correction	Multi-scan	Multi-scan	Multi-scan
<i>T_{min}</i>	0.967	0.957	0.936
<i>T_{max}</i>	0.980	0.991	0.987
No. of measured, independent and observed reflections	8093, 1511, 1232	10 780, 1503, 1222	7771, 1653, 1519
Criterion for observed reflections	<i>I</i> > 2σ(<i>I</i>)	<i>I</i> > 2σ(<i>I</i>)	<i>I</i> > 2σ(<i>I</i>)
<i>R_{int}</i>	0.034	0.043	0.031
θ_{\max} (°)	27.5	27.5	27.5
Range of <i>h</i> , <i>k</i> , <i>l</i>	–10 ⇒ <i>h</i> ⇒ 11 –7 ⇒ <i>k</i> ⇒ 8 –15 ⇒ <i>l</i> ⇒ 15	–9 ⇒ <i>h</i> ⇒ 10 –19 ⇒ <i>k</i> ⇒ 19 –8 ⇒ <i>l</i> ⇒ 8	–10 ⇒ <i>h</i> ⇒ 10 –8 ⇒ <i>k</i> ⇒ 9 –15 ⇒ <i>l</i> ⇒ 14
Refinement			
Refinement on	<i>F</i> ²	<i>F</i> ²	<i>F</i> ²
<i>R</i> [<i>F</i> ² > 2σ(<i>F</i> ²)], <i>wR</i> (<i>F</i> ²), <i>S</i>	0.039, 0.124, 1.00	0.060, 0.160, 1.02	0.040, 0.107, 1.25
No. of reflections	1511	1503	1653
No. of parameters	100	100	199
H-atom treatment	Constrained to parent site	Constrained to parent site	Constrained to parent site
Weighting scheme	$w = 1/[\sigma^2(F_o^2) + (0.093P)^2 + 0.0092P]$, where $P = (F_o^2 + 2F_c^2)/3$	$w = 1/[\sigma^2(F_o^2) + (0.0754P)^2 + 0.8974P]$, where $P = (F_o^2 + 2F_c^2)/3$	$w = 1/[\sigma^2(F_o^2) + (0.0658P)^2 + 0.0096P]$, where $P = (F_o^2 + 2F_c^2)/3$
(Δ/σ) _{max}	<0.0001	<0.0001	<0.0001
$\Delta\rho_{\max}$, $\Delta\rho_{\min}$ (e Å ⁻³)	0.23, –0.29	1.44, –0.31	0.27, –0.31
	(III)	(IV)	(V)
Crystal data			
Chemical formula	C ₁₄ H ₁₀ N ₄ O ₄	C ₁₄ H ₁₀ N ₄ O ₄	C ₁₄ H ₁₀ N ₄ O ₄
<i>M_r</i>	298.26	298.26	298.26
Cell setting, space group	Monoclinic, <i>P2₁/n</i>	Monoclinic, <i>C2/c</i>	Monoclinic, <i>P2₁/n</i>
Temperature (K)	120 (2)	120 (2)	120 (2)
<i>a</i> , <i>b</i> , <i>c</i> (Å)	7.0128 (4), 7.6318 (5), 12.8037 (5)	30.865 (3), 4.7660 (5), 21.736 (2)	3.7318 (2), 7.2442 (3), 23.9367 (10)
β (°)	105.825 (3)	123.926 (2)	94.053 (2)
<i>V</i> (Å ³)	659.29 (6)	2653.1 (5)	645.48 (5)
<i>Z</i>	2	8	2
<i>D_x</i> (Mg m ⁻³)	1.502	1.493	1.535
Radiation type	Mo <i>K</i> α	Synchrotron	Mo <i>K</i> α
No. of reflections for cell parameters	1507	2789	1479
θ range (°)	3.1–27.6	3.0–28.8	2.9–27.6
μ (mm ⁻¹)	0.11	0.11	0.12
Crystal form, colour	Plate, yellow	Lath, yellow	Lath, yellow
Crystal size (mm)	0.43 × 0.30 × 0.08	0.10 × 0.06 × 0.01	0.40 × 0.10 × 0.01
Data collection			
Diffraction	Bruker–Nonius 95 mm CCD camera on κ goniostat	Bruker SMART APEX2 CCD diffractometer	Bruker–Nonius 95 mm CCD camera on κ goniostat
Data collection method	φ and ω scans	Fine-slice ω scans	φ and ω scans
Absorption correction	Multi-scan	Multi-scan	Multi-scan

Table 1 (continued)

	(III)	(IV)	(V)
T_{\min}	0.969	0.980	0.949
T_{\max}	0.991	0.999	0.999
No. of measured, independent and observed reflections	7854, 1507, 1095	14 589, 3961, 2817	6443, 1479, 1239
Criterion for observed reflections	$I > 2\sigma(I)$	$I > 2\sigma(I)$	$I > 2\sigma(I)$
R_{int}	0.061	0.034	0.049
θ_{max} (°)	27.6	29.0	27.6
Range of h, k, l	$-9 \Rightarrow h \Rightarrow 9$ $-9 \Rightarrow k \Rightarrow 9$ $-16 \Rightarrow l \Rightarrow 14$	$-43 \Rightarrow h \Rightarrow 44$ $-6 \Rightarrow k \Rightarrow 6$ $-30 \Rightarrow l \Rightarrow 30$	$-4 \Rightarrow h \Rightarrow 4$ $-9 \Rightarrow k \Rightarrow 9$ $-30 \Rightarrow l \Rightarrow 31$
Refinement			
Refinement on	F^2	F^2	F^2
$R[F^2 > 2\sigma(F^2)]$, $wR(F^2)$, S	0.044, 0.122, 1.04	0.057, 0.170, 1.09	0.041, 0.110, 1.06
No. of reflections	1507	3961	1479
No. of parameters	100	199	100
H-atom treatment	Constrained to parent site	Constrained to parent site	Constrained to parent site
Weighting scheme	$w = 1/[\sigma^2(F_o^2) + (0.068P)^2 + 0.1014P]$, where $P = (F_o^2 + 2F_c^2)/3$	$w = 1/[\sigma^2(F_o^2) + (0.095P)^2 + 1.033P]$, where $P = (F_o^2 + 2F_c^2)/3$	$w = 1/[\sigma^2(F_o^2) + (0.0454P)^2 + 0.3185P]$, where $P = (F_o^2 + 2F_c^2)/3$
$(\Delta/\sigma)_{\text{max}}$	<0.0001	0.001	0.001
$\Delta\rho_{\text{max}}, \Delta\rho_{\text{min}}$ (e Å ⁻³)	0.20, -0.35	0.44, -0.26	0.24, -0.24

Computer programs used: COLLECT (Hooft, 1999), APEX2 (Bruker AXS Inc., 2004), DENZO (Otwinowski & Minor, 1997), SAINT (Bruker AXS Inc., 2004), OSCAIL (McArdle, 2003), SHELXS97 (Sheldrick, 1997), SHELXL97 (Sheldrick, 1997), PLATON (Spek, 2003), PRPKAPPA (Ferguson, 1999), SADABS (Sheldrick, 2003).

Table 2
Selected torsional angles (°).

(a) Centrosymmetric isomers				
Parameter	(Ia)	(Ib)	(III)	(V)
N1 ⁱ –N1–C7–C1	-176.75 (11)	-176.8 (2)	-179.28 (14)	179.48 (13)
N1–C7–C1–C2	-146.55 (12)	-149.4 (2)	-3.0 (2)	178.82 (13)
C1–C2–N2–O21	19.17 (15)	21.2 (3)	–	–
C2–C3–N3–O31	–	–	-3.83 (19)	–
C3–C4–N4–O41	–	–	–	9.71 (19)
(b) Non-centrosymmetric isomers				
Parameter	(II)	(IV)		
C17–N11–N21–C27	175.13 (18)	-172.53 (14)		
N21–N11–C17–C11	-179.66 (18)	-179.43 (13)		
N11–C17–C11–C12	-159.7 (2)	6.4 (2)		
N11–N21–C27–C21	179.39 (17)	-178.92 (14)		
N21–C27–C21–C22	165.11 (19)	-175.28 (15)		
C11–C12–N12–O121	25.1 (3)	–		
C22–C23–N23–O231	-3.9 (3)	–		
C12–C13–N13–O131	–	-1.5 (2)		
C23–C24–N24–O241	–	-0.1 (2)		

Symmetry code: (i) $1 - x, 1 - y, 1 - z$.

Supramolecular analyses were made and the diagrams were prepared with the aid of PLATON (Spek, 2003). Details of molecular conformations are given in Table 2, and details of hydrogen-bond dimensions are given in Table 3.¹

3. Results and discussion

3.1. Molecular conformations

In the symmetrically substituted isomers (I), (III) and (V), the molecules lie across centres of inversion, and in all of the

¹ Supplementary data for this paper are available from the IUCr electronic archives (Reference: BM5032). Services for accessing these data are described at the back of the journal.

Table 3
Selected hydrogen-bond parameters (Å, °).

D–H...A	H...A	D...A	D–H...A
(Ib)			
C3–H3...Cg1 [†]	2.89	3.568 (2)	129
(II)			
C14–H14...O232 ⁱⁱ	2.45	3.178 (3)	134
C22–H22...O231 ⁱⁱⁱ	2.51	3.289 (3)	139
(III)			
C4–H4...O32 ^{iv}	2.50	3.448 (2)	176
(IV)			
C14–H14...O132 ^v	2.44	3.309 (3)	151
C17–H17...O242 ^{vi}	2.42	3.262 (2)	147
C22–H22...O131 ^{viii}	2.51	3.363 (3)	149
C27–H27...O131 ^{viii}	2.53	3.383 (2)	149
(V)			
C3–H3...O41 ^{viii}	2.50	3.186 (2)	129
C7–H7...O42 ^{ix}	2.47	3.343 (2)	152

Symmetry codes: (i) $x, \frac{3}{2} - y, -\frac{1}{2} + z$; (ii) $1 + x, 2 + y, z$; (iii) $1 - x, \frac{1}{2} + y, 1 - z$; (iv) $-1 - x, -y, 1 - z$; (v) $1 - x, -2 - y, 1 - z$; (vi) $\frac{3}{2} - x, \frac{3}{2} - y, 1 - z$; (vii) $1 - x, 1 + y, \frac{1}{2} - z$; (viii) $\frac{3}{2} - x, -\frac{1}{2} + y, \frac{3}{2} - z$; (ix) $1 + x, -1 + y, z$. [†] Cg1 is the centroid of ring C1–C6.

isomers the central C=C=N–N=C–C fragment has an all-transoid conformation and it is essentially planar, as shown by the leading torsional angles (Table 2). In both polymorphs of (I), where there is a 2-nitro substituent, the aryl rings are significantly twisted out of the plane of the central spacer unit, and the molecular conformations are very similar, as shown by the leading torsional angles (Table 2). However, in isomers (III) and (V), containing 3-nitro and 4-nitro substituents, respectively, the aryl rings are almost coplanar with the spacer unit. In (III) the nitro group is on the edge of the molecule remote from the methine C–H bond, whereas in both polymorphs of (I) the two groups are on the same edge (Table 2;

Figs. 1, 2 and 4). In isomer (II) both of the independent nitro groups are on the same edges of the molecules as the nearest methine C—H bond, whereas the 3-nitro group in isomer (IV) is remote from the corresponding C—H bond (Table 2; Figs. 3 and 5). In all of compounds (I)–(V), the bond lengths and angles present no unusual features.

3.2. Supramolecular aggregation

3.2.1. Polymorphs of isomer (I), 1,4-bis(2-nitrophenyl)-2,3-diaza-1,3-butadiene. The supramolecular aggregation of the two polymorphs (*Ia*) and (*Ib*) of isomer (I) differs significantly: the supramolecular aggregation is determined in (*Ia*) by an aromatic $\pi \cdots \pi$ stacking interaction and in (*Ib*) by a C—H $\cdots \pi$ (arene) hydrogen bond: $\pi \cdots \pi$ stacking interactions are absent from the structure of (*Ib*).

The aryl rings in (*Ia*) at (x, y, z) and $(-x, 2 - y, 1 - z)$ are components of the molecules across the inversion centres at $(0.5, 0.5, 0.5)$ and $(-0.5, 1.5, 0.5)$, respectively. These two rings are strictly parallel with an interplanar spacing of 3.569 (2) Å; the ring-centroid separation is 3.887 (2) Å, corresponding to a nearly ideal centroid offset of 1.539 (2) Å. Propagation by inversion of this interaction then leads to the formation of a π -stacked chain of centrosymmetric molecules running parallel to the $[1\bar{1}0]$ direction (Fig. 7).

In polymorph (*Ib*) the chain structure is generated by a single C—H $\cdots \pi$ (arene) hydrogen bond (Table 3). The aryl C3 atom in the ring at (x, y, z) is part of the molecule centred across $(\frac{1}{2}, \frac{1}{2}, \frac{1}{2})$: this atom acts as a hydrogen-bond donor to the aryl ring at $(x, \frac{3}{2} - y, -\frac{1}{2} + z)$, which forms part of the molecule centred across $(\frac{1}{2}, 1, 0)$. Propagation of this hydrogen bond then forms a zigzag chain running parallel to the $[01\bar{1}]$ direction and generated by the *c*-glide plane at $y = 0.75$ (Fig. 8). In the structures of both (*Ia*) and (*Ib*) two chains pass through

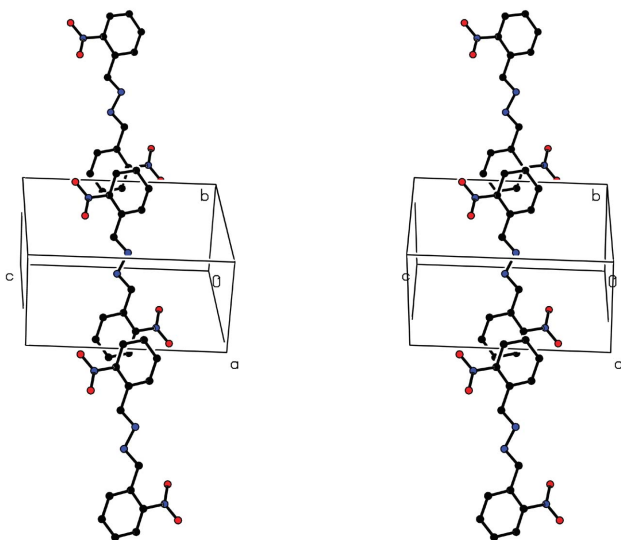


Figure 7
Stereoview of part of the crystal structure of polymorph (*Ia*) showing the formation of a π -stacked chain along $[1\bar{1}0]$. For the sake of clarity the H atoms have all been omitted.

each unit cell, but there are no direction-specific interactions between adjacent chains.

3.2.2. Isomer (II), 1-(2-nitrophenyl)-4-(3-nitrophenyl)-2,3-diaza-1,3-butadiene. In contrast to the dimorphism observed for (I), only a single polymorph has been observed for the isomeric 1-(2-nitrophenyl)-4-(3-nitrophenyl)-2,3-diazabutadiene (II) (Fig. 3). In this isomer the molecules lie in general positions in the non-centrosymmetric space group $P2_1$, but the molecular skeleton apart from the nitro groups is nearly centrosymmetric, as shown by the principal torsional angles (Table 2).

The two-dimensional supramolecular structure of isomer (II) is built from two independent C—H \cdots O hydrogen bonds (Table 3), augmented by a $\pi \cdots \pi$ stacking interaction: C—H $\cdots \pi$ (arene) hydrogen bonds are absent, however. The aryl C22 atom in the molecule at (x, y, z) acts as a hydrogen-bond donor to the nitro O231 atom in the molecule at $(1 - x, \frac{1}{2} + y, 1$

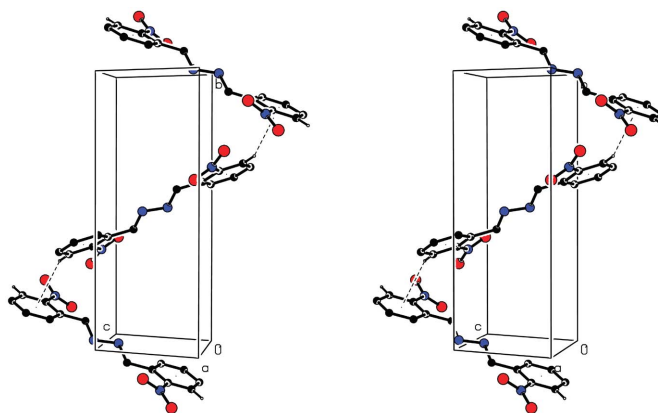


Figure 8
Stereoview of part of the crystal structure of polymorph (*Ib*) showing the formation of a hydrogen-bonded chain along $[01\bar{1}]$. For the sake of clarity the H atoms not involved in the motif shown have been omitted.

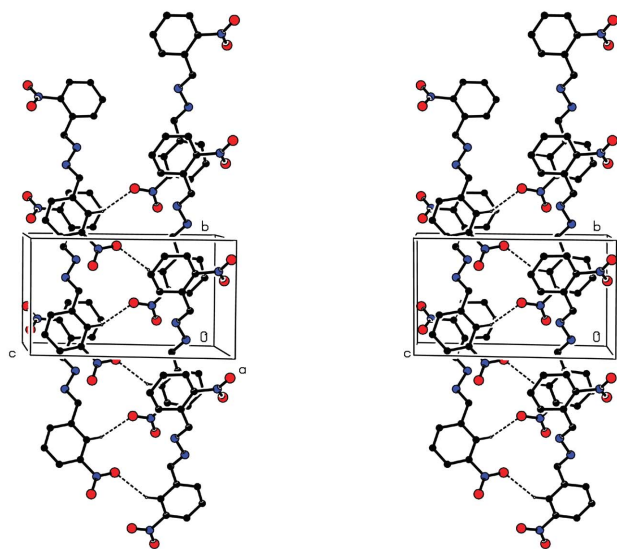


Figure 9
Stereoview of part of the crystal structure of isomer (II) showing the formation of a hydrogen-bonded C(5) chain along $[010]$. For the sake of clarity the H atoms not involved in the motif shown have been omitted.

$-z$), so forming a spiral $C(5)$ chain (Bernstein *et al.*, 1995) running parallel to the $[010]$ direction and generated by the 2_1 screw axis along $(\frac{1}{2}, y, \frac{1}{2})$ (Fig. 9). At the same time, the aryl C14 atom in the molecule at (x, y, z) acts as a hydrogen-bond donor to the nitro O232 atom in the molecule at $(1+x, 2+y, z)$, so generating by translation a $C(14)$ chain running parallel to the $[120]$ direction (Fig. 10). It is notable that the two O acceptor atoms in (II) belong to the same nitro group: the second nitro group containing the N12 atom plays no part in the hydrogen bonding. The combination of the $[101]$ and $[120]$ chains generates a (001) sheet, which is reinforced by the $\pi \cdots \pi$ stacking interaction.

The aryl rings C11–C16 and C21–C26 in the molecules at (x, y, z) and $(1+x, 1+y, z)$, respectively, make a dihedral angle of only $1.1(2)^\circ$. The ring–centroid separation is $3.722(2) \text{ \AA}$ and the interplanar spacing is *ca* 3.42 \AA , corresponding to a centroid offset of *ca* 1.48 \AA . In this manner a $[110]$ chain is produced (Fig. 11), which lies wholly within the hydrogen-bonded (001) sheet. There are no direction-specific interactions between adjacent sheets.

3.2.3. Isomer (III), 1,4-bis(3-nitrophenyl)-2,3-diaza-1,3-butadiene. The molecules of the 3,3' isomer (III) (Fig. 4) lie across centres of inversion in the space group $P2_1/n$ with the reference molecule selected as that lying across $(\frac{1}{2}, \frac{1}{2}, \frac{1}{2})$. The molecules are effectively planar, and they are linked into chains of rings by a single $C-H \cdots O$ hydrogen bond (Table 3), and the chains are further linked into sheets by a single $\pi \cdots \pi$ stacking interaction. The aryl C4 atom at (x, y, z) , which lies in the molecule centred at $(\frac{1}{2}, \frac{1}{2}, \frac{1}{2})$, acts as a hydrogen-bond donor to the nitro O32 atom at $(-1-x, -y, 1-z)$, which lies in the molecule centred at $(-\frac{3}{2}, -\frac{1}{2}, \frac{1}{2})$: propagation by inversion of this single hydrogen bond then generates a $C(14)[R_2^2(10)]$ chain of rings running parallel to the $[210]$ direction (Fig. 12).

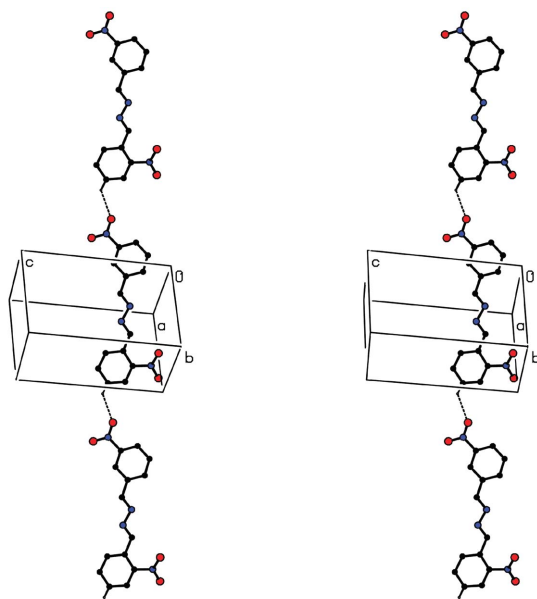


Figure 10
Stereoview of part of the crystal structure of isomer (II) showing the formation of a hydrogen-bonded $C(14)$ chain along $[120]$. For the sake of clarity the H atoms not involved in the motif shown have been omitted.

The aryl rings at (x, y, z) and $(-x, -y, 1-z)$, which form parts of the molecules of (III) centred at $(\frac{1}{2}, \frac{1}{2}, \frac{1}{2})$ and $(-\frac{1}{2}, -\frac{1}{2}, \frac{1}{2})$, respectively, are strictly parallel with an interplanar spacing of $3.344(2) \text{ \AA}$; the ring–centroid separation is $3.784(2) \text{ \AA}$, corresponding to a ring offset of $1.770(2) \text{ \AA}$. Propagation by inversion of this π -stacking interaction then generates a chain running parallel to the $[110]$ direction (Fig. 13). The combination of $[110]$ and $[210]$ chains generates a (001) sheet, but there are no direction-specific interactions between adjacent sheets.

3.2.4. Isomer (IV), 1-(3-nitrophenyl)-4-(4-nitrophenyl)-2,3-diaza-1,3-butadiene. Although the molecules of the 3,4'

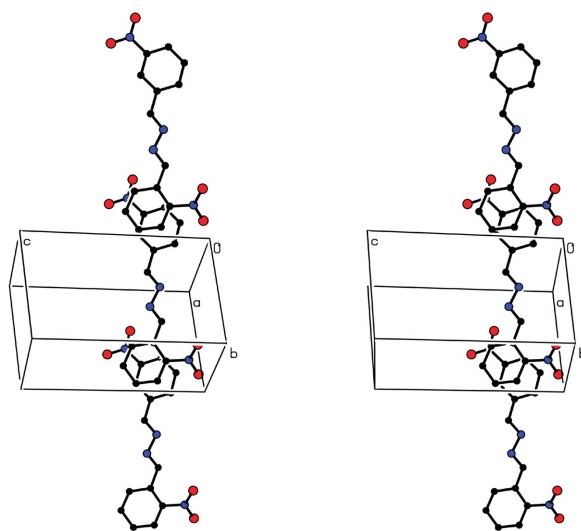


Figure 11
Stereoview of part of the crystal structure of isomer (II) showing the formation of a π -stacked chain along $[110]$. For the sake of clarity the H atoms have all been omitted.

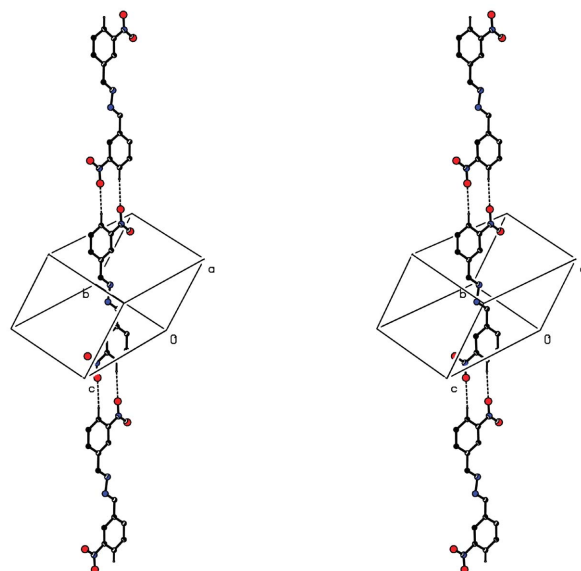


Figure 12
Stereoview of part of the crystal structure of isomer (III) showing the formation of a hydrogen-bonded chain of rings along $[210]$. For the sake of clarity the H atoms not involved in the motif shown have been omitted.

isomer (IV) (Fig. 5) have no crystallographic symmetry, nonetheless they are very nearly planar. The two-dimensional aggregation is determined by four C—H...O hydrogen bonds (Table 3), but it can readily be analysed in terms of two one-dimensional substructures. In the first of these substructures, the aryl C14 atom in the molecule at (x, y, z) acts as a hydrogen-bond donor to the nitro O132 atom in the molecule at $(1 - x, -2 - y, 1 - z)$, thereby forming an $R_2^2(10)$ ring centred at $(\frac{1}{2}, -1, \frac{1}{2})$; similarly, the methine C17 atom at (x, y, z) acts as a donor to the nitro O242 atom in the molecule at $(\frac{3}{2} - x, \frac{3}{2} - y, 1 - z)$, so forming an $R_2^2(22)$ ring centred at $(\frac{3}{4}, \frac{3}{4}, \frac{1}{2})$. Propagation by inversion of these two interactions then

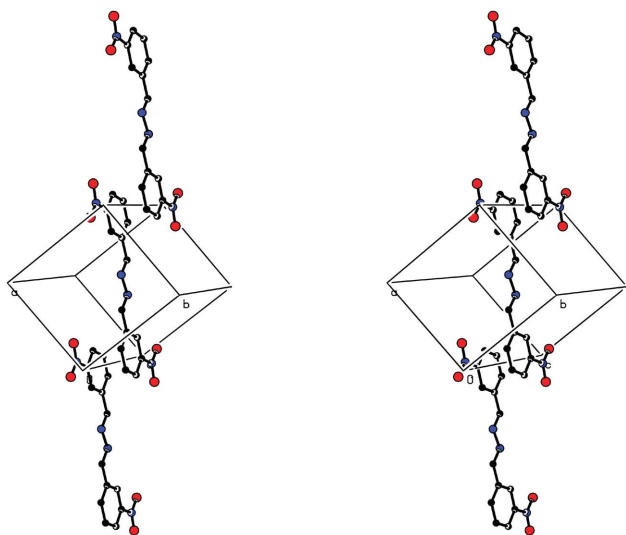


Figure 13
Stereoview of part of the crystal structure of isomer (III) showing the formation of a π -stacked chain along $[110]$. For the sake of clarity the H atoms have been omitted.

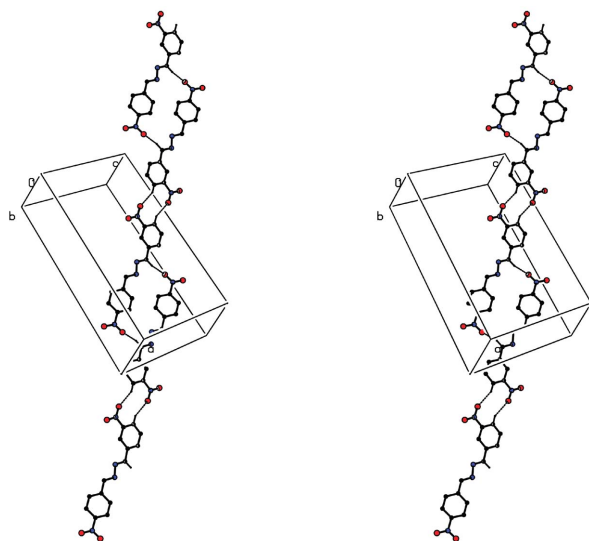


Figure 14
Stereoview of part of the crystal structure of isomer (IV) showing the formation of a chain along $[170]$ containing $R_2^2(10)$ and $R_2^2(22)$ rings. For the sake of clarity the H atoms not involved in the motif shown have been omitted.

generates a $C_2^2(22)[R_2^2(10)][R_2^2(22)]$ chain of rings running parallel to the $[170]$ direction (Fig. 14). In the second substructure, atoms C22 and C27 in the molecule at (x, y, z) both act as donors to the nitro O131 atom in the molecule at $(1 - x, 1 + y, \frac{1}{2} - z)$, while C22 and C27 at $(1 - x, 1 + y, \frac{1}{2} - z)$ in turn act as donors to O131 at $(x, 2 + y, z)$. In this way a pair of $C(10)C(12)[R_2^2(6)]$ chains of rings (Fig. 15) is generated by the twofold rotation axis along $(\frac{1}{2}, y, \frac{1}{4})$, forming a double helix running parallel to the $[010]$ direction (Fig. 16). The combination of the $[170]$ and $[010]$ chains generates a (001) sheet.

3.2.5. Isomer (V), 1,4-bis(4-nitrophenyl)-2,3-diaza-1,3-butadiene. The molecules of the 4,4' isomer (V) (Fig. 6) lie across centres of inversion in the space group $P2_1/n$ with the reference molecule selected as that lying across $(\frac{1}{2}, \frac{1}{2}, \frac{1}{2})$. With the exception of the nitro groups, the molecules are effectively planar (Table 2). The supramolecular aggregation in (V) is dominated by two C—H...O hydrogen bonds, one much stronger than the other (Table 3). The overall effect of these

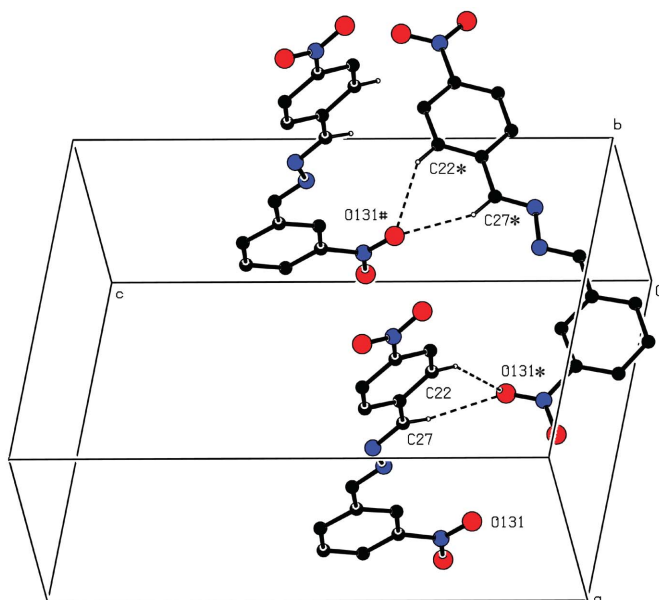


Figure 15
Part of the crystal structure of isomer (IV) showing the formation of a $[010]$ chain of rings along $[010]$. For the sake of clarity the H atoms not involved in the motif shown have been omitted. The atoms marked with an asterisk (*) or a hash (#) are at the symmetry positions $(1 - x, 1 + y, \frac{1}{2} - z)$ and $(x, 2 + y, z)$, respectively.

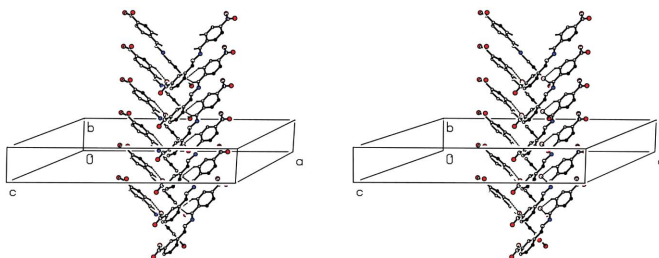


Figure 16
Stereoview of part of the crystal structure of isomer (IV), showing the formation of a hydrogen-bonded double helix along $[010]$. For the sake of clarity the H atoms not involved in the motif shown have been omitted.

interactions is to link the molecules into a three-dimensional framework, and the formation of this framework is most readily analysed in terms of two substructures, each generated by a single hydrogen bond. In the stronger interaction, the methine C7 atom at (x, y, z) acts as a hydrogen-bond donor to the nitro O41 atom at $(1 + x, -1 + y, z)$: propagation of this interaction by translation and inversion then leads to the formation of a chain of edge-fused centrosymmetric $R_2^2(22)$ rings running parallel to the $[1\bar{1}0]$ direction (Fig. 17).

In contrast to the stronger hydrogen bond, which generates a one-dimensional substructure, the weaker interaction generates a substructure which is two-dimensional. The aryl atoms C3 at (x, y, z) and $(1 - x, 1 - y, 1 - z)$, which both form part of the molecule centred at $(\frac{1}{2}, \frac{1}{2}, \frac{1}{2})$, act as hydrogen-bond donors, respectively, to the nitro O41 atoms at $(\frac{3}{2} - x, -\frac{1}{2} + y, \frac{3}{2} - z)$ and $(-\frac{1}{2} + x, \frac{3}{2} - y, -\frac{1}{2} + z)$, which themselves lie in the molecules centred at $(1, 0, 1)$ and $(0, 1, 0)$, respectively. Similarly, the O41 atoms at (x, y, z) and $(1 - x, 1 - y, 1 - z)$ accept hydrogen bonds from C3 atoms at $(\frac{3}{2} - x, \frac{1}{2} + y, \frac{3}{2} - z)$ and $(-\frac{1}{2} + x, \frac{1}{2} - y, -\frac{1}{2} + z)$, respectively, which are components of the molecules centred at $(1, 1, 1)$ and $(0, 0, 0)$, respectively. Propagation of this hydrogen bond then generates a $(10\bar{1})$ sheet in the form of a $(4, 4)$ net (Batten & Robson, 1998) built from a single type of $R_4^4(38)$ ring (Fig. 18). The combination of the $[110]$ chains and $(10\bar{1})$ sheets suffices to link all of the molecules into a single framework, from which C—H... π (arene) hydrogen bonds and aromatic π ... π stacking interactions are, however, both absent.

3.2.6. General discussion of the structures. In making comparisons between the supramolecular aggregation patterns of the various forms of bis(nitrobenzaldehyde)azine, it is convenient to consider firstly the symmetrically substi-

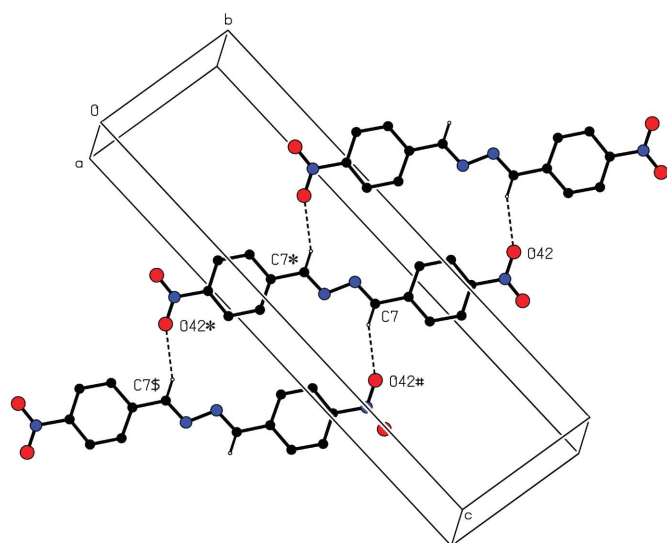


Figure 17

Part of the crystal structure of isomer (V) showing the formation of a chain of edge-fused $R_2^2(22)$ rings along $[110]$. For the sake of clarity the H atoms not involved in the motif shown have been omitted. The atoms marked with an asterisk (*), a hash (#) or a dollar sign (\$) are at the symmetry positions $(1 - x, 1 - y, 1 - z)$, $(1 + x, -1 + y, z)$ and $(2 - x, -y, 1 - z)$, respectively.

tuted isomers and then the non-symmetric forms. The supramolecular structures of the two polymorphs (*Ia*) and (*Ib*) of the 2,2'-isomer are both one-dimensional (Figs. 7 and 8), but they depend upon different intermolecular interactions, π ... π stacking in (*Ia*) and a C—H... π (arene) hydrogen bond in (*Ib*). In the 3,3'-isomer (III) the supramolecular structure is two-dimensional, utilizing a C—H...O hydrogen bond and a π ... π stacking interaction, while in the 4,4'-isomer (V) the only direction-specific intermolecular interactions are two independent C—H...O hydrogen bonds which generate a three-dimensional structure. Thus, these symmetrical isomers can form supramolecular structures which are one-, two- or three-dimensional, and in which no two exhibit the same types of intermolecular interaction.

Amongst the three non-symmetrically substituted isomers, the 2,3'-isomer (II) forms a two-dimensional supramolecular structure dominated by two C—H...O hydrogen bonds, and the structure of the 3,4'-isomer (IV) is again two-dimensional but here determined by four independent C—H...O hydrogen bonds.

Within the two- and three-dimensional structures a wide variety of low-dimensional substructures can be discerned, including simple chains in the 2,3'-isomer (II) (Figs. 9 and 10), chains of rings in both the 3,3'-isomer (III) and the 3,4'-isomer (IV), including a double-helical chain in (IV) (Figs. 12, 14, 15 and 16), and both chains of edge-fused rings and sheets of $R_4^4(38)$ rings in the 4,4'-isomer (V) (Figs. 17 and 18).

These supramolecular structures are built from C—H...O and C—H... π (arene) hydrogen bonds and aromatic π ... π stacking interactions although, perhaps surprisingly, C—H...N hydrogen bonds are absent. All of these interactions are comparatively weak; accordingly, the computational modelling and prediction of crystal structures in which interactions of this type are the only direction-specific intermolecular interactions present, is fraught with difficulty. Despite considerable effort in recent years, reliable predictive methods for such structures remain elusive: extended series of isomeric compounds, such as those whose structures are described here, will provide a keen test of computational methods for structure prediction.

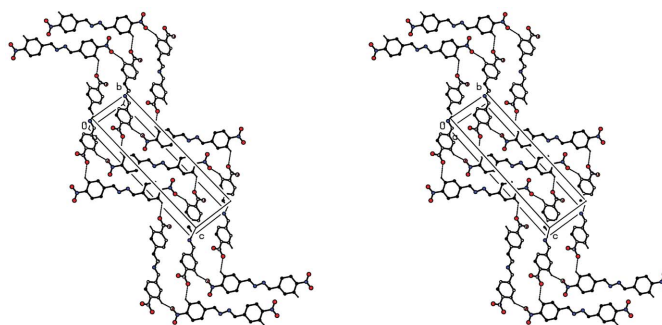


Figure 18

Stereoview of part of the crystal structure of isomer (V) showing the formation of a sheet of $R_4^4(38)$ rings parallel to $(10\bar{1})$. For the sake of clarity the H atoms not involved in the motif shown have been omitted.

4. Concluding remarks

The supramolecular structures of (Ia), (Ib) and (II)–(V) all exhibit different combinations of direction-specific intermolecular interactions, and different overall patterns of supramolecular aggregation. Accordingly it is not possible to make a reliable prediction of the supramolecular molecular structure of isomer (VI). To the extent that no one structure in this series can be predicted, even with knowledge of all the others, the series under study here neatly mimics the behaviour of other extended series of simple positional isomers which we have studied recently, including iodo-arene-nitroarenesulfonamides (Kelly *et al.*, 2002), nitrobenzylidene-iodoanilines, where solvent-dependent polymorphism occurs (Glidewell, Howie *et al.*, 2002; Ferguson *et al.*, 2005), iodo-*N*-(nitrobenzyl)anilines (Glidewell, Low *et al.*, 2002) and *N*-iodophenyl)nitrophthalimides (Glidewell, Low, Skakle, Wardell & Wardell, 2005). In each of these series, every isomer manifests a distinct pattern of intermolecular interactions such that predictions on further isomers become merely speculative. The occurrence of polymorphism in two of these series adds to the overall complexity, which presents a keen challenge to computational methods for crystal structure prediction.

X-ray data were collected at the EPSRC X-ray Crystallographic Service, University of Southampton, UK, and at the Daresbury SRS station 9.8: the authors thank the staff of these facilities for all their help and advice. JLW thanks CNPq and FAPERJ for financial support.

References

- Batten, S. R. & Robson, R. (1998). *Angew. Chem. Int. Ed.* **37**, 1460–1494.
- Bernstein, J., Davis, R. E., Shimon, L. & Chang, N.-L. (1995). *Angew. Chem. Int. Ed. Engl.* **34**, 1555–1573.
- Bruker AXS Inc. (2004). *APEX2* and *SAINT*, Version 6.02. Bruker AXS Inc., Madison, Wisconsin, USA.
- Ferguson, G. (1999). *PRPKAPPA – a WordPerfect-5.1 Macro to Formulate and Polish CIF Format Files from the SHELXL-97 Refinement of Kappa-CCD Data*. University of Guelph, Canada.
- Ferguson, G., Glidewell, C., Low, J. N., Skakle, J. M. S. & Wardell, J. L. (2005). *Acta Cryst.* **C61**, o445–o449.
- Flack, H. D. (1983). *Acta Cryst.* **A39**, 876–881.
- Flack, H. D. & Bernardinelli, G. (2000). *J. Appl. Cryst.* **33**, 1143–1148.
- Glidewell, C., Howie, R. A., Low, J. N., Skakle, J. M. S., Wardell, S. M. S. V. & Wardell, J. L. (2002). *Acta Cryst.* **B58**, 864–876.
- Glidewell, C., Low, J. N., Skakle, J. M. S. & Wardell, J. L. (2005). *Acta Cryst.* **C61**, o312–o316.
- Glidewell, C., Low, J. N., Skakle, J. M. S., Wardell, S. M. S. V. & Wardell, J. L. (2002). *Acta Cryst.* **C58**, o487–o490.
- Glidewell, C., Low, J. N., Skakle, J. M. S., Wardell, S. M. S. V. & Wardell, J. L. (2005). *Acta Cryst.* **B61**, 227–237.
- Hooft, R. W. W. (1999). *Collect. Nonius BV*, Delft, The Netherlands.
- Hsu, L.-Y., Nordman, C. E. & Kenny, D. H. (1993). *Acta Cryst.* **C49**, 394–398.
- Jones, P. G. (1986). *Acta Cryst.* **A42**, 57.
- Kelly, C. J., Skakle, J. M. S., Wardell, J. L., Wardell, S. M. S. V., Low, J. N. & Glidewell, C. (2002). *Acta Cryst.* **B58**, 94–108.
- McArdle, P. (2003). *OSCAIL for Windows*. Version 10. Crystallography Centre, Chemistry Department, NUI Galway, Ireland.
- Otwinowski, Z. & Minor, W. (1997). *Methods in Enzymology*, Vol. 276, *Macromolecular Crystallography*, Part A, edited by C. W. Carter Jr & R. M. Sweet, pp. 307–326. New York: Academic Press.
- Sheldrick, G. M. (1997). *SHELXS97* and *SHELXL97*. University of Göttingen, Germany.
- Sheldrick, G. M. (2003). *SADABS*. Version 2.10. University of Göttingen, Germany.
- Spek, A. L. (2003). *J. Appl. Cryst.* **36**, 7–13.
- Wilson, A. J. C. (1976). *Acta Cryst.* **A32**, 994–996.